ChemComm

COMMUNICATION

View Article Online
View Journal

Cite this: DOI: 10.1039/d0cc07989h

Received 8th December 2020,
Accepted 15th April 2021

DOI: 10.1039/d0cc07989h

rsc.li/chemcomm

Permanently polarized hydroxyapatite for selective electrothermal catalytic conversion of carbon dioxide into ethanol†

Jordi Sans,[a] Guillem Revilla-López,[a] Vanesa Sanz,[b] Jordi Puiggalí,[ac] Pau Turon *[b] and Carlos Alemán *[acd]

Conversion of CO_2 into valuable chemicals is not only a very challenging topic but also a socially demanding issue. In this work, permanently polarized hydroxyapatite obtained using a thermal stimulated polarization process is proposed as a highly selective catalyst for green production of ethanol starting from CO_2 and CH_4.

Carbon dioxide (CO_2) is considered the primary greenhouse gas and the main cause of global climate warming. Therefore, its efficient utilization as a C1 feedstock to synthesize high value chemical and industrial products, such as carbon monoxide,[1–3] methanol,[4–6] ethanol,[7–9] formic acid,[10–12] ureas,[13] and carbonates,[14,15] among others, is drawing increasing attention. Transition metals and, more recently, complexes that can act as transition metals dominate the catalysis associated with CO_2 activation and fixation.[16–19] However, environmentally friendly, simpler and cheaper catalysts are highly desirable. Moreover, there is an urgent demand for engineering and manufacturing catalysts for CO_2 recycling under mild conditions (*i.e.* <10 bar pressure and <250 °C temperature) with lower levels of environmental contamination and reduced cost.

Hydroxyapatite (HAp) is a naturally occurring mineral form of calcium apatite, exhibiting similarity with human hard tissues in morphology and composition. Polarized HAp (p-HAp), which is obtained by applying a thermally stimulated polarization process to HAp,[20,21] presents electrocatalytic behaviour due to its capacitive and electrochemical properties.[22] Herein, we report the use of such a bioceramic catalyst, p-HAp, for CO_2 fixation under mild conditions, affording a selective catalytic synthesis of ethanol that involves hydrogenation of reduced CO_2 and C–C bond construction as well.

HAp was prepared by the hydrothermal method using $(NH_4)_2HPO_4$ and $Ca(NO_3)_2$ as reagents. The obtained samples were sintered for 2 h at 1000 °C in air and, subsequently, polarized by applying 3 kV cm^{-1} at 1000 °C for 1 h. The success of the polarization process is proved in Fig. S1 (ESI†), which compares the Raman ν_1 peak in the 930–990 cm^{-1} interval before and after HAp polarization. Thermally stimulated polarization produces an improvement in the definition of the vibrational modes and a reduction of the full width at half maximum (FWHM) from 9 cm^{-1} to 5 cm^{-1}. This fact is consistent with a reduction of HAp crystal imperfections and a decrease in the content of amorphous calcium phosphate and β-tricalcium phosphate phases. Additionally, p-HAp was confirmed through other previously described electrical and structural assays, which are routinely conducted to distinguish the polarized catalyst from non-polarized HAp (np-HAp).[20,21]

p-HAp can be described as nanoparticles of approximately 100–300 nm that aggregate forming agglomerates of up to 1 μm in size (Fig. 1a). Additional characterization of p-HAp by wide angle X-ray diffraction (WAXD), high-resolution transmission electron microscopy (HRTEM) and X-ray photoelectron spectroscopy (XPS) is provided in Fig. S2–S4 (ESI†). Recently, we reported a multi-component electrophotocatalyst made of p-HAp coated with zirconyl chloride, which hydrolyses into zirconia under reaction conditions, and aminotris(methylenephosphonic acid) (ATMP).[22,23] The catalyst, hereafter named p-HAp/coat, yielded glycine and alanine (D/L racemic mixture) by fixing nitrogen from N_2 and carbon from CO_2 and CH_4 at 95 °C and 1 bar. The molar yield of amino acids was duplicated when the pressure increased up to 6 bar, maintaining the temperature at 95 °C. Conversely, amino acids were not formed when p-HAp was replaced by np-HAp and/or when the coating was not deposited onto the surface of p-HAp.

[a] Departament d'Enginyeria Química and Barcelona Research Center for Multiscale Science and Engineering, Universitat Politècnica de Catalunya, EEBE, C/Eduard Maristany 10-14, 08019 Barcelona, Spain. E-mail: carlos.aleman@upc.edu
[b] Research and Development. B. Braun Surgical, S.A.U., Carretera de Terrasa 121, 08191 Rubí (Barcelona), Spain. E-mail: pau.turon@bbraun.com
[c] Institute for Bioengineering of Catalonia (IBEC), The Barcelona Institute of Science and Technology, Baldiri Reixac 10-12, 08028 Barcelona, Spain
[d] Laboratory of the Environmental Center (LCMA), Universitat Politècnica Pau Turon de Catalunya, EEBE, C/Eduard Maristany 10-14, 08019 Barcelona, Spain

† Electronic supplementary information (ESI) available: Experimental procedures, Raman spectra and ^1H NMR spectra are included in the supporting information. See DOI: 10.1039/d0cc07989h

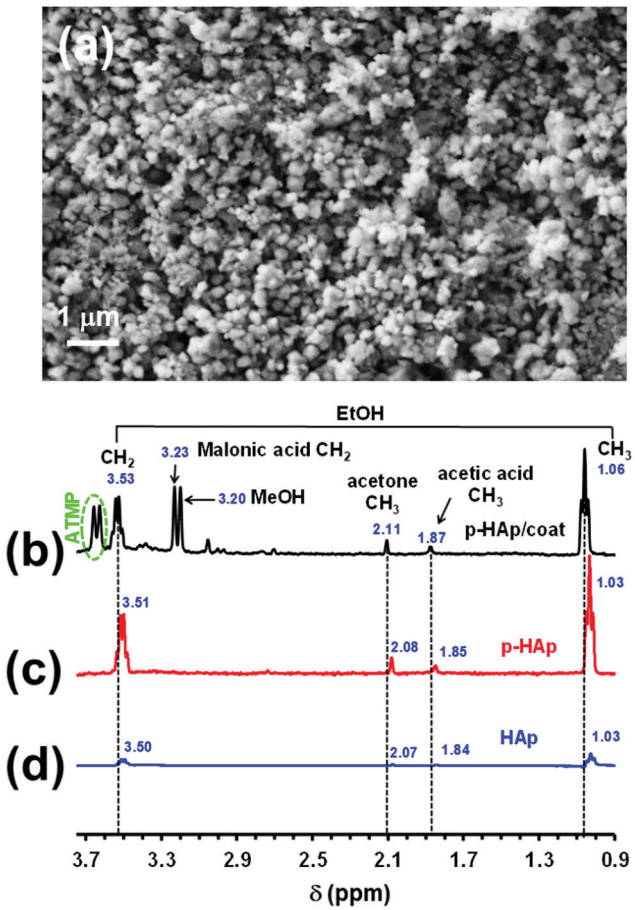

Fig. 1 (a) Scanning electron microscopy micrograph of p-HAp. (b–d) ^{1}H NMR spectra of the solutions obtained by dissolving the catalysts after the reaction: (b) p-HAp/coat, (c) p-HAp and (d) HAp. The reactions in (b–d) were conducted for 72 h using CO_2 (3 bar), CH_4 (3 bar) and H_2O (1 mL) at 95 °C under UV radiation.

In this work a carbon fixation reaction was catalysed by p-HAp/coat in an inert reaction chamber using a CO_2 and CH_4 gas mixture (3 bar each) and liquid H_2O (1 mL) under irradiation of an UV lamp illuminating directly the catalyst at 95 °C. Fig. 1b shows the ^{1}H-NMR spectrum obtained after 72 h reaction from the catalyst dissolved in deuterated water containing 100 mM HCl and 50 mM NaCl, which allowed us to identify the following reaction products on the surface of the catalyst (yields expressed as μmol of product per gram of catalyst): ethanol (16.1 ± 3.2 μmol g^{-1}), methanol (4.9 ± 1.0 μmol g^{-1}), malonic acid (1.6 ± 0.2 μmol g^{-1}), acetone (0.8 ± 0.2 μmol g^{-1}) and acetic acid (0.6 ± 0.1 μmol g^{-1}). The predominant product, ethanol was identified by the quartet (CH_2) and the triplet (CH_3) at 3.53 and 1.06 ppm, respectively, since the OH peak at 4.65 ppm overlapped with the intense water band (Fig. S5, ESI†). The selectivity, expressed as the ratio of ethanol to the rest of the products, was 2.0, while the conversion of CO_2 and CH_4 into products was 0.08%.

In the synthesis of amino acids, the role attributed to the different components of the p-HAp/coat catalyst can be broken down as follows: p-HAp is an electrocatalyst due to its electrical properties, electrochemical activity and ability to store charge; zirconia is a well-known photocatalyst with a relatively wide band gap value and high negative value of the conduction band potential,[24–26] which was found to be essential for fixation of nitrogen from N_2; and ATMP weakly attracts the N_2 molecules towards the surface of the catalysts.[22,23] In order to confirm the electrocatalyzed fixation of the CO_2, the zirconia and ATMP coatings were eliminated from the catalyst. Analysis of the reaction products obtained directly using p-HAp under the same experimental conditions led to (Fig. 1c): ethanol (19.4 ± 3.8 μmol g^{-1}), acetone (0.9 ± 0.1 μmol g^{-1}) and acetic acid (0.6 ± 0.1 μmol g^{-1}). This represents a 20% increment in the yield of ethanol, while methanol and malonic acid were not detected. The selectivity increased from 2.0 to 12.9, while the conversion of feeding gases into products decreased to 0.07%. Moreover, the influence of the polarization process on the catalytic activity of conventional (non-polarized) HAp is proved in Fig. 1d, which only produced a very low amount of ethanol (1.9 ± 0.5 μmol g^{-1} catalyst) under the same reaction conditions (*i.e.* yields of acetone and acetic acid were <0.1 μmol g^{-1} catalyst). In the absence of any solid support acting as a catalyst (negative control 1 in Fig. S6, ESI†), the yield of ethanol was practically null ($<0.1 \pm 0.05$ μmol g^{-1}). Such a small amount, which was attributed to eventual photo-induced CO_2 reduction and water splitting, totally disappeared in the absence of UV radiation (negative control 2 in Fig. S6, ESI†).

Chemical shifts observed after the dissolution of the p-HAp/coat were slightly de-shielded with respect to the peaks of products derived from p-HAp (Fig. 1b–d). This effect was attributed to the ATMP, which increased the acidity of the medium, causing downfield shifts that are not detected for p-HAp and HAp, independently of the conditions (Fig. 1). On the other hand, the elimination of the coating from the catalyst not only increases the conversion into ethanol by 20% but also maximizes its selective synthesis of ethanol as the major reaction product (from 67% to 93%). This was attributed to the fact that the exposed surface is greater and the surface charge distribution is more homogeneous for p-Hap than for p-HAp/coat.[23]

In order to explore the role of the UV radiation and electrochemical activity imparted by the polarization process in the reaction catalyzed by p-HAp, the process was repeated without UV illumination at 95 °C (Fig. 2a and b). The yield of ethanol decreased drastically, from 19.4 ± 3.8 to 0.2 ± 0.03 μmol g^{-1}, while acetone and acetic acid were not detected. By increasing the temperature to 140 °C, which is the maximum temperature allowed by the reactor, the yield of ethanol, acetone and acetic acid increased up to 17.8 ± 1.8, 0.9 ± 0.2 and 0.7 ± 0.1 μmol g^{-1} catalysts, respectively, these values being very similar to those achieved by using UV radiation and 95 °C (Fig. 2c). This feature indicates that the thermally activated electrocatalytic CO_2 conversion predominates over the photocatalytic reaction and that UV radiation can be used to lower the free energy barrier to form intermediates once CO_2 is adsorbed onto the catalyst surface. Moreover, the selectivity towards ethanol at 140 °C without UV radiation was 11.1. Accordingly, the whole of the results

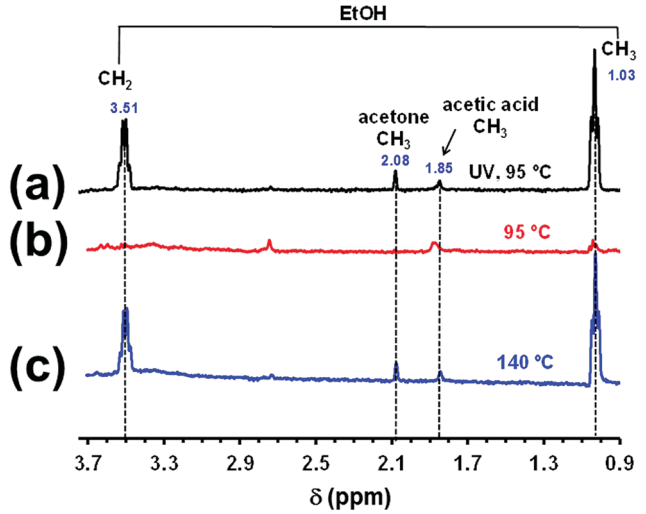

Fig. 2 ^{1}H NMR spectra of the solutions obtained by dissolving the catalysts after the reaction. All the reactions were conducted for 72 h using CO_2 (3 bar), CH_4 (3 bar) and H_2O (1 mL), p-HAp as catalyst, and the following specific conditions: (a) 95 °C under UV radiation; (b) 95 °C without UV radiation; and (c) 140 °C without UV radiation.

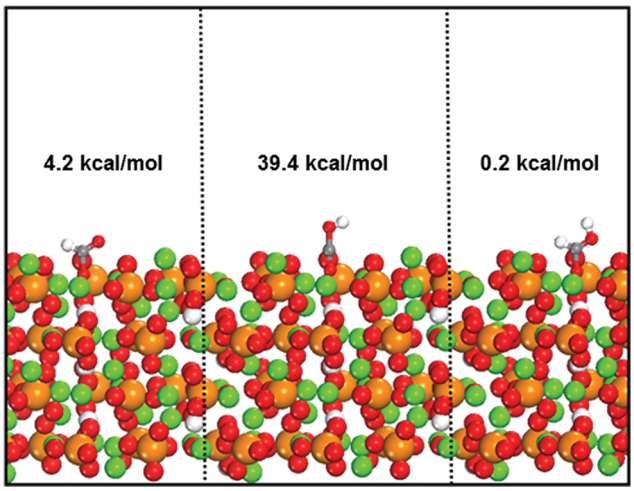

Fig. 3 Representative protonated forms of CO_2 adsorbed molecules on the OH^- vacancy of the p-HAp. Numerical values (in eV) stand for the calculated adsorption energies.

obtained using p-HAp/coat and p-HAp catalysts, which were achieved using different experimental conditions (*i.e.* 95 and 140 °C and with/without UV radiation) indicate that the selective conversion of CO_2 into ethanol is due to an electrothermal catalytic process. It should be noted that thermal activation is necessary due to the fact that the capacitive behaviour of p-HAp, which is a ceramic, is much lower than that of conventional metallic electrocatalysts.[20] Furthermore, comparison of the Raman spectra of p-HAp before and after the reaction demonstrates the structural stability of the catalyst, which remains unaltered (Fig. S7, ESI†).

In order to support the p-HAp fixation mechanism based on the formation of carboxylates, DFT calculations were performed at the PBE-D3 level. The (0001) facet, which is the most stable HAp surface,[27] and an isodesmic model in which H_2 is used as a source of protons were considered for the calculations. Adsorption energies for different protonation products of CO_2 were calculated by inserting the molecules in the hydroxyl vacancy of the mineral. The results proved that the protonation of CO_2 to yield formic acid is exothermic in the gas phase by -3.1 kcal mol^{-1} but it is more exothermic when adsorbed on p-HAp substrate, by -32.7 kcal mol^{-1}. Yet, all protonated species displayed endothermic adsorption energies; the one for the protonated formic acid was very small (0.2 kcal mol^{-1}) while the one for CO_2 was 5.1 kcal mol^{-1}. Other adsorption sites were checked on the p-HAp displaying higher energies (Fig. 3), thus making this pathway unfeasible to be followed completely and shifting the catalysis location elsewhere close to the surface but not directly adsorbed.

Analysis of the liquid water incorporated into the reaction chamber (Fig. S8, ESI†) provided additional information on the total yield and confirmed that the catalytic reaction takes place over the p-HAp surface, supporting the theoretically proposed pathway. Interestingly, an additional small amount of ethanol (0.7 ± 0.1 μmol g^{-1}) and acetic acid (2.0 ± 0.5 μmol g^{-1}), which probably converts into acetone on the catalyst surface, formic acid (1.9 ± 0.6 μmol g^{-1}) and methanol (1.5 ± 0.3 μmol g^{-1}) can be identified as well. This feature suggests that both the CO_2 activation and the formation of the reduced $^*COO^-$ intermediate do not occur on the surface of the solid catalyst but close to it. Thus, when the intermediate incorporates water, which is in contact with the p-HAp catalyst, it does not evolve towards ethanol but protonates to yield formic acid. Finally, methanol can be originated as a result of the $^*CH_3$ radicals trapped in water or from formic acid. In any case, the impact of the reaction products dissolved in the water phase on the ethanol selectivity is negligible.

The reaction with p-HAp at 95 °C and UV radiation was repeated considering the two following scenarios: (i) complete absence of water; and (ii) an excess of initial water (20 mL) in the reactor. In the latter case, the catalyst was partially immersed in water and, during the reaction, a water vapor rich atmosphere was expected. The results show how the regulation of the initial amount of water is very important for the efficient reduction of CO_2 (Fig. S9, ESI†). Although both ethanol and acetone were obtained in the absence of water, their yield was very low (4.7 ± 0.9 and 0.1 ± 0.06 μmol g^{-1}, respectively) in comparison to that achieved when 1 mL of water was introduced in the reaction chamber. This difference was attributed to the difficulties in generating and stabilizing active radical species in the catalyst when it is dry (*i.e.* only with water absorbed from atmospheric moisture). On the other hand, the excess of water also caused a notable reduction in the yield of ethanol and acetone (7.0 ± 0.1 and 0.3 ± 0.07 μmol g^{-1}, respectively), which again were the only products that are formed. However, in this case the low yield was associated with the fact that the water saturated atmosphere makes gas exchange more difficult at the hydrophilic catalyst interface.

As a proof of concept the reaction was repeated at atmospheric pressure using contaminated air taken from the

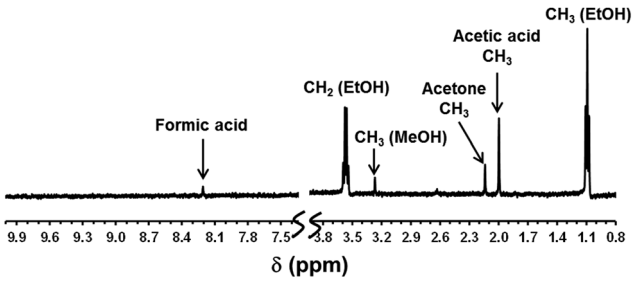

Fig. 4 ^{1}H NMR spectrum of the solution obtained by dissolving the catalyst. The reaction was conducted for 72 h using polluted air (atmospheric pressure), H_2O (1 mL), and p-HAp as a catalyst at 95° under UV radiation.

surrounding area of the UPC East Campus in Barcelona, an area heavily polluted by car traffic since it is in front of one of the main roads of the city. The contaminated air by combustion of fossil carburant contains significantly higher CO_2 and CH_4 than the average of the ambient air. The reaction was conducted using p-HAp, in the presence of 1 mL of water and at 95 °C with UV radiation. Analysis of the reaction products after 72 h showed ethanol and other products (Fig. 4), some of them identified in previous reactions with controlled gas mixtures, such as methanol, acetone, acetic acid and formic acid. Despite the fact that the amount of ethanol was very small (1.1 ± 0.2 μmol g^{-1}), it was found to be the predominant reaction product, confirming the potential applicability of p-HAp to regenerate contaminated air while obtaining added value subproducts as ethanol.

In summary, we demonstrate the selective catalytic activity of p-HAp to convert gaseous CO_2 into ethanol. The selective yield of ethanol achieved in this work (~90%) is among the highest reported in the literature, in which a wide range of values (from 60% to 93%) were described.[28] On the other hand, the CO_2 conversion achieved with the bioceramic catalyst (~0.08%) is lower than those reported for metallic-based catalysts (*e.g.* Cu), even though these usually worked at higher pressures.[29] For example, Cu^{I}@Zr_{12}-bpdc exhibited a conversion of 0.5% at 20 bar, while Zr_{12}-bpdc-CuCs showed a conversion of 52% at 40 bar. Both theoretical calculations and experiments under different reaction conditions provide important insights about the mechanism pathway. As a proof of concept, the proposed reaction has been successful in obtaining ethanol from road traffic contaminated air, opening an exciting new avenue to transform greenhouse gas emissions into valuable chemical products using a simple catalyst based on an earth-abundant mineral.

The authors acknowledge MINECO/FEDER (RTI2018-098951-B-I00 and RTI2018-101827-B-I00), the Agència de Gestió d'Ajuts Universitaris i de Recerca (2017SGR359 and 2017SGR373) and B. Braun for financial support. Support for the research of C.A. by ICREA Academia program for excellence in research is gratefully acknowledged.

Conflicts of interest

The authors declare that the preparation and application of permanently polarized hydroxyapatite as a catalyst was patented by the Universitat Politcnica de Catalunya and B Braun Surgical S.A. (EP16382381, EP16382524, P27990EP00, PCT/EP2017/069437, and P58656 EP).

Notes and references

1 H. X. Zhong, M. Ghorbani-Asl, K. H. Ly, J. C. Zhang, J. Ge, M. C. Wang, Z. Q. Kiao, D. Marakov, E. Zschech, E. Brunner, I. M. Widinger, J. Zhang, A. V. Krashinnikov, S. Laskel, R. H. Dong and X. L. Feng, *Nat. Commun.*, 2020, **11**, 1409.
2 C. Cometto, R. Kuriki, L. Chen, K. Maeda, T. C. Lau, O. Ishitani and M. A. Robert, *J. Am. Chem. Soc.*, 2018, **140**, 7437–7440.
3 Y. Wang, J. Liu, Y. Wang, Y. Wang and G. Zheng, *Nat. Commun.*, 2018, **9**, 5003.
4 S. Kar, R. Sen, A. Goeppert and G. K. S. Prakash, *J. Am. Chem. Soc.*, 2018, **140**, 1580–1583.
5 Y. Wang, X. Liu, X. Y. Han, R. Godin, J. L. Chen, W. Z. Zhou, C. R. Jiang, J. F. Thompson, K. B. Mustafa, S. A. Shevlin, J. R. Durrant, Z. X. Guo and J. W. Tang, *Nat. Commun.*, 2020, **11**, 2531.
6 W. Zhang, Y. Hu, L. Ma, G. Zhu, Y. Wang, X. Xue, R. Chen, S. Yang and Z. Jin, *Adv. Sci.*, 2018, **5**, 1700275.
7 J. Du, S. P. Li, S. L. Liu, Y. Xin, B. F. Chen, H. Z. Liu and B. X. Han, *Chem. Sci.*, 2020, **11**, 5098–5104.
8 B. An, Z. Li, Y. Song, J. Z. Zhang, L. Z. Zeng, C. Wang and W. B. Lin, *Nat. Catal.*, 2019, **2**, 709–717.
9 M. C. Luo, Z. Y. Wang, Y. G. C. Li, J. Li, F. W. Li, Y. W. Lum, D. H. Nam, B. Chen, J. Wicks, A. N. Xu, T. T. Zhuang, W. R. Leow, X. Wang, C. T. Dinh, Y. Wang, Y. H. Wang, D. Sinton and E. H. Sargent, *Nat. Commun.*, 2019, **10**, 5814.
10 T. X. Zhao, X. B. Hu, Y. T. Wu and Z. B. Zhang, *Angew. Chem., Int. Ed.*, 2019, **58**, 722–726.
11 A. Weilhard, M. I. Qadir, V. Sans and J. Dupont, *ACS Catal.*, 2018, **8**, 1628–1634.
12 B. Kumar, V. Atla, J. P. Brian, S. Kumari, T. Q. Nguyen, M. Sunkara and J. M. Spurgeon, *Angew. Chem., Int. Ed.*, 2017, **56**, 3645–3649.
13 J. Hwang, D. Han, J. J. Oh, M. Cheong, H. J. Koo, J. S. Lee and H. S. Kim, *Adv. Synth. Catal.*, 2019, **361**, 297–306.
14 S. Dabral, U. Licht, P. Rudolf, G. Bollmann, A. S. K. Hashmi and T. Schaub, *Green Chem.*, 2020, **22**, 1553–1558.
15 A. J. Kamphuis, F. Picchioni and P. P. Pescarmona, *Green Chem.*, 2019, **21**, 406–448.
16 Z. H. Li, L. Zhang, M. Nishiura, G. Luo, Y. Luo and Z. M. Hou, *J. Am. Chem. Soc.*, 2020, **142**, 1966–1974.
17 C. S. Yeung, *Angew. Chem., Int. Ed.*, 2019, **58**, 5492–5502.
18 P. P. Power, *Nature*, 2010, **463**, 171–177.
19 D. D. Zhu, J. L. Liu and S. Z. Qiao, *Adv. Mater.*, 2016, **28**, 3423–3452.
20 M. Rivas, L. J. del Valle, E. Armelin, O. Betran, P. Turon, J. Puiggalí and C. Alemán, *ChemPhysChem*, 2018, **19**, 1746–1755.
21 J. Sans, J. Llorca, V. Sanz, J. Puiggalí and C. Alemán, *Langmuir*, 2019, **35**, 14782–14790.
22 M. Rivas, L. J. del Valle, P. Turon, C. Alemán and J. Puiggalí, *Green Chem.*, 2018, **20**, 685–693.
23 J. Sans, E. Armelin, V. Sanz, J. Puiggalí, P. Turon and C. Alemán, *J. Catal.*, 2020, **389**, 646–656.
24 P. Bansal, G. R. Chaudhary and S. K. Mehta, *Chem. Eng. J.*, 2015, **280**, 475–485.
25 T. Sreethawong, S. Ngamsinlapasathian and S. Yoshikawa, *Chem. Eng. J.*, 2013, **228**, 256–262.
26 H. Zheng, K. Y. Liu, H. Q. Cao and X. R. Zhang, *J. Phys. Chem. C*, 2009, **113**, 18259–18263.
27 D. Mkhonto and N. H. De Leeuw, *J. Mater. Chem.*, 2002, **12**, 2633–2642.
28 L. Fan, C. Xia, F. Yang, J. Wang, H. Wang and Y. Lu, *Adv. Sci.*, 2020, **6**, eaay3111.
29 B. An, Z. Li, Y. Song, J. Zhang, L. Zeng, C. Wang and W. Lin, *Nat. Catal.*, 2019, **2**, 709–717.

